

Accelerated Articles**Implementation of Electron-Transfer Dissociation on a Hybrid Linear Ion Trap–Orbitrap Mass Spectrometer**Graeme C. McAlister,[†] Doug Phanstiel,[†] David M. Good,[†] W. Travis Berggren,[‡] and Joshua J. Coon^{*,†,§}

Departments of Chemistry and Biomolecular Chemistry, University of Wisconsin, Madison, Wisconsin 53706, and WiCell Research Institute, Madison, Wisconsin 53706

We describe the adaptation of a hybrid quadrupole linear ion trap–orbitrap mass spectrometer to accommodate electron-transfer ion/ion reactions (ETD) for peptide and protein characterization. The method utilizes pulsed, dual electrospray ion sources and requires minimal instrument modification. Switching between cation and reagent anion injection schemes is automated and accomplished within a few hundred milliseconds. Ion/ion reactions are conducted within the linear ion trap, after which the c- and z-type product ions are passed to the orbitrap for high-resolution m/z analysis. With this arrangement, mass accuracies are typically measured to within 2 ppm at a resolving power of $\sim 60\,000$. Using large peptides and intact proteins, we demonstrate such capabilities will accelerate our ability to interrogate high-mass species. To illustrate compatibility with automated data-dependent analysis and subsequent data processing, we couple the technique with an online chromatographic separation of a yeast whole-cell lysate followed by peptide identification using ProSight PC. Fairly long pulsing times and relatively low ET efficiency, as compared to conventional ETD instrumentation, are the main drawbacks of this approach. Still, our results suggest that the implementation of ETD on sensitive, high-resolution, and high-mass accuracy hybrid instrumentation, such as the orbitrap, will substantially propel the emergent fields of middle- and top-down proteomics.

Because it extends electron capture-like fragmentation (ECD) to more common bench top tandem mass spectrometer systems,

* To whom correspondence should be addressed: E-mail: jcoon@chem.wisc.edu.

electron-transfer dissociation (ETD) has generated considerable interest in the field of proteomic research.^{1–3} The utility of the technique to localize post-translational modifications (PTMs), its relative indifference to amino acid composition or order, and capacity to randomly dissociate large peptide and even whole protein cations on a chromatographic time scale make it the perfect complement to conventional collision-activated methodology (CAD).^{4–8} Still, because they are generated within the context of a radio frequency (rf) ion trap, ETD-type product ions are almost exclusively mass analyzed with low m/z resolution and accuracy (i.e., that typically achieved with ion trap devices). Doubtless ion trap MS systems offer a splendid format for conducting ion/ion reactions,^{9–13} but such m/z resolution and accuracy limitations

[†] Department of Chemistry, University of Wisconsin.

[‡] WiCell Research Institute.

[§] Biomolecular Chemistry, University of Wisconsin.

- (1) Good, D. M.; Coon, J. J. *Biotechniques* **2006**, *40*, 783–789.
- (2) Coon, J. J.; Syka, J. E. P.; Schwartz, J. C.; Shabanowitz, J.; Hunt, D. F. *Int. J. Mass Spectrom.* **2004**, *236*, 33–42.
- (3) Syka, J. E. P.; Coon, J. J.; Schroeder, M. J.; Shabanowitz, J.; Hunt, D. F. *Proc. Natl. Acad. Sci. U.S.A.* **2004**, *101*, 9528–9533.
- (4) Gunawardena, H. P.; Emory, J. F.; McLuckey, S. A. *Anal. Chem.* **2006**, *78*, 3788–3793.
- (5) Hogan, J. M.; Pitteri, S. J.; Chrisman, P. A.; McLuckey, S. A. *J. Proteome Res.* **2005**, *4*, 628–632.
- (6) Pitteri, S. J.; Chrisman, P. A.; Hogan, J. M.; McLuckey, S. A. *Anal. Chem.* **2005**, *77*, 1831–1839.
- (7) Coon, J. J.; Ueberheide, B.; Syka, J. E. P.; Dryhurst, D. D.; Ausio, J.; Shabanowitz, J.; Hunt, D. F. *Proc. Natl. Acad. Sci. U.S.A.* **2005**, *102*, 9463–9468.
- (8) Swaney, D. L.; McAlister, G. C.; Wirtala, M.; Schwartz, J. C.; Syka, J. E. P.; Coon, J. J. *Anal. Chem.* **2007**, *79*, 477–485.
- (9) Herron, W. J.; Goeringer, D. E.; McLuckey, S. A. *Anal. Chem.* **1996**, *68*, 257–262.
- (10) Stephenson, J. L.; McLuckey, S. A. *Int. J. Mass Spectrom.* **1997**, *165*, 419–431.
- (11) Stephenson, J. L.; McLuckey, S. A. *Int. J. Mass Spectrom. Ion Processes* **1997**, *162*, 89–106.

have restricted the practice of ETD. Linear quadrupole ion traps (QLT), however, are increasingly used as intermediate storage chambers, mass analyzers, or both on a number of hybrid MS systems—e.g., quadrupole time-of-flight (Qq-TOF), linear ion trap Fourier transform-ion cyclotron resonance (QLT-FT-ICR), and most recently linear ion trap-orbitrap (QLT-orbitrap).^{7,13–17} Adaptation of such hybrid instrumentation to accommodate ETD is of obvious utility, but has been technically challenging to realize.

In the initial implementation of ETD, we fitted a negative chemical ionization source (NCI) to the unoccupied end of a QLT system.³ The NCI source generated anions of polyaromatic hydrocarbons like anthracene or fluoranthene, which were then injected into the rear side of the QLT for reaction with a population of previously isolated peptide cations. For the instruments noted above, both sides of the QLT are occupied—the front with the cation injection optics and the rear with a second analyzer. Thus, because it demands substantial mechanical design and alteration, incorporation of an NCI source on these types of hybrids has yet to be reported. Just this year, McLuckey and colleagues have proposed a second option for the implementation of ETD on hybrid instrumentation—dual atmospheric pressure ionization (API) sources (referred to herein as front end-ETD, FE-ETD). In their first approach, a nanoelectrospray (nESI) probe for peptide cation generation is complemented with an atmospheric pressure chemical ionization (APCI) source for anion generation—both are located on the front end of a triple quadrupole system and more recently a Qq-TOF.^{18,19} Cyclic operation of the two sources permitted sequential injection of discrete cation and anion populations, and APCI-generated anions of nitrobenzene and azobenzene were shown to induce ETD with varying degrees of efficiency. A significant concern regarding the viability of this approach is the necessity for ambient volatilization of the anion reagent molecule. Azobenzene, for example, is a common pesticide and known carcinogen.

In their second FE-ETD approach, McLuckey et al. described a clever strategy for the preparation of ETD-inducing anions via ESI.²⁰ In general, anions formed by ESI are expected to have high electron affinities and will only react with peptide cations via proton transfer.⁴ This report demonstrated that 9-anthracenecarboxylic acid could be generated using ESI and subsequently decarboxylated via CAD to render an ETD-capable anion—the same anion created by NCI of anthracene in the initial description of ETD.³ These experiments were performed on a custom QIT having multiple independent atmospheric pressure sources so that both

cation and anion populations were generated continuously with gating performed by downstream ion optics. ESI reagent anion generation eliminates the ambient volatilization issues associated with APCI and offers an attractive route for the implementation of ETD on hybrid instrumentation.

Here we extend this dual ESI source concept for implementing ETD reactions on a single-inlet QLT-orbitrap hybrid mass spectrometer. Nearby, but independent, nanospray emitters are pulsed on and off (~200-ms time scale) to generate discrete populations of ions for subsequent ion/ion reactions in the QLT. Following ETD, product ions are injected into the orbitrap mass analyzer in the normal fashion and high-resolution and mass accuracy product ion spectra are acquired. The process has sufficient efficiency to permit single-scan orbitrap product ion mass spectra where c- and z-type product ion m/z values are recorded to within 2 ppm mass accuracies. We demonstrate this approach will dramatically propel our ability to characterize large peptides and even whole proteins by analyzing intact ubiquitin cations and a complex peptide mixture with online chromatographic separations.

MATERIALS AND METHODS

Sample Preparation. All peptides, proteins, and chemicals were obtained from Sigma-Aldrich (St. Louis, MO) unless otherwise noted. The peptide KAAAKAAK was synthesized at the University of Wisconsin Biotechnology Center (Madison, WI). Peptide and protein solutions were prepared by dilution of stock solutions to ~3 pmol/ μ L in 60:39.9:0.1 (v/v/v) acetonitrile/water/acetic acid. The reagent anion 9-anthracenecarboxylic acid was dissolved in a solution of 50:50 (v/v) acetonitrile/water to a concentration of 150 μ mol/ μ L. This solution was centrifuged (~9000 rcf) for ~5 min to prevent particulates from clogging the nESI tip during infusion.

Instrumentation. Unless otherwise noted, all the data shown were collected on a modified LTQ-orbitrap hybrid mass spectrometer (Thermo Electron, Bremen, Germany). First, the QLT of the hybrid instrument was adapted to apply an rf trapping voltage to the end lenses of the linear trap (Figure 1). By applying rf voltages in both the radial (applied to the quadrupole rods) and axial (applied to the end lenses) directions without additional dc offsets, ions of opposing charge can be trapped in the same space at the same time (i.e., charge-sign independent trapping, CSIT). The first ETD-compatible instrument utilized a QLT modified for CSIT—these changes are detailed more thoroughly elsewhere.³ Second, the orbitrap was modified to accommodate an additional high-voltage supply to power a second nESI emitter—which was directly interfaced to the ion trap control hardware. This modification allowed control of both ion source power supplies through the instrument software. Analyte precursor cations and reagent anions were generated using independent, commercially available static nano ESI tips (New Objective, Woburn MA). The nanospray emitters were held in proximity to the atmospheric pressure inlet (Figure 1) using a modified Thermo Electron nanospray source. Each tip was connected to one of the aforementioned high voltage (–8 to 8 kV) power supplies. Rather than turn the supplies on and off during each scan event, the voltage set points were pulsed high (± 1 –2 kV) or low (0 V)—a process that took ~200 ms.

At the beginning of each scan event, the cation emitter power supply was set high (~1.2 kV) to establish cation analyte nESI.

- (12) McLuckey, S. A.; Stephenson, J. L. *Mass Spectrom. Rev.* **1998**, *17*, 369–407.
- (13) Syka, J. E. P.; Marto, J. A.; Bai, D. L.; Horning, S.; Senko, M. W.; Schwartz, J. C.; Ueberheide, B.; Garcia, B.; Busby, S.; Muratore, T.; Shabanowitz, J.; Hunt, D. F. *J. Proteome Res.* **2004**, *3*, 621–626.
- (14) Thevis, M.; Makarov, A. A.; Horning, S.; Schanzer, W. *Rapid Commun. Mass Spectrom.* **2005**, *19*, 3369–3378.
- (15) Michael, S. M.; Chien, B. M.; Lubman, D. M. *Anal. Chem.* **1993**, *65*, 2614–2620.
- (16) Verentchikov, A. N.; Ens, W.; Standing, K. G. *Anal. Chem.* **1994**, *66*, 126–133.
- (17) Shevchenko, A.; Loboda, A.; Shevchenko, A.; Ens, W.; Standing, K. G. *Anal. Chem.* **2000**, *72*, 2132–2141.
- (18) Liang, X.; Xia, Y.; McLuckey, S. A. *Anal. Chem.* **2006**, *78*, 3208–3212.
- (19) Xia, Y.; Chrisman, P. A.; Erickson, D. E.; Liu, J.; Liang, X.; Londry, F. A.; Yang, M. J.; McLuckey, S. A. *Anal. Chem.* **2006**, *78*, 4146–4154.
- (20) Huang, T. Y.; Emory, J. F.; O'Hair, R. A.; McLuckey, S. A. *Anal. Chem.* **2006**, *78*, 7387–7391.

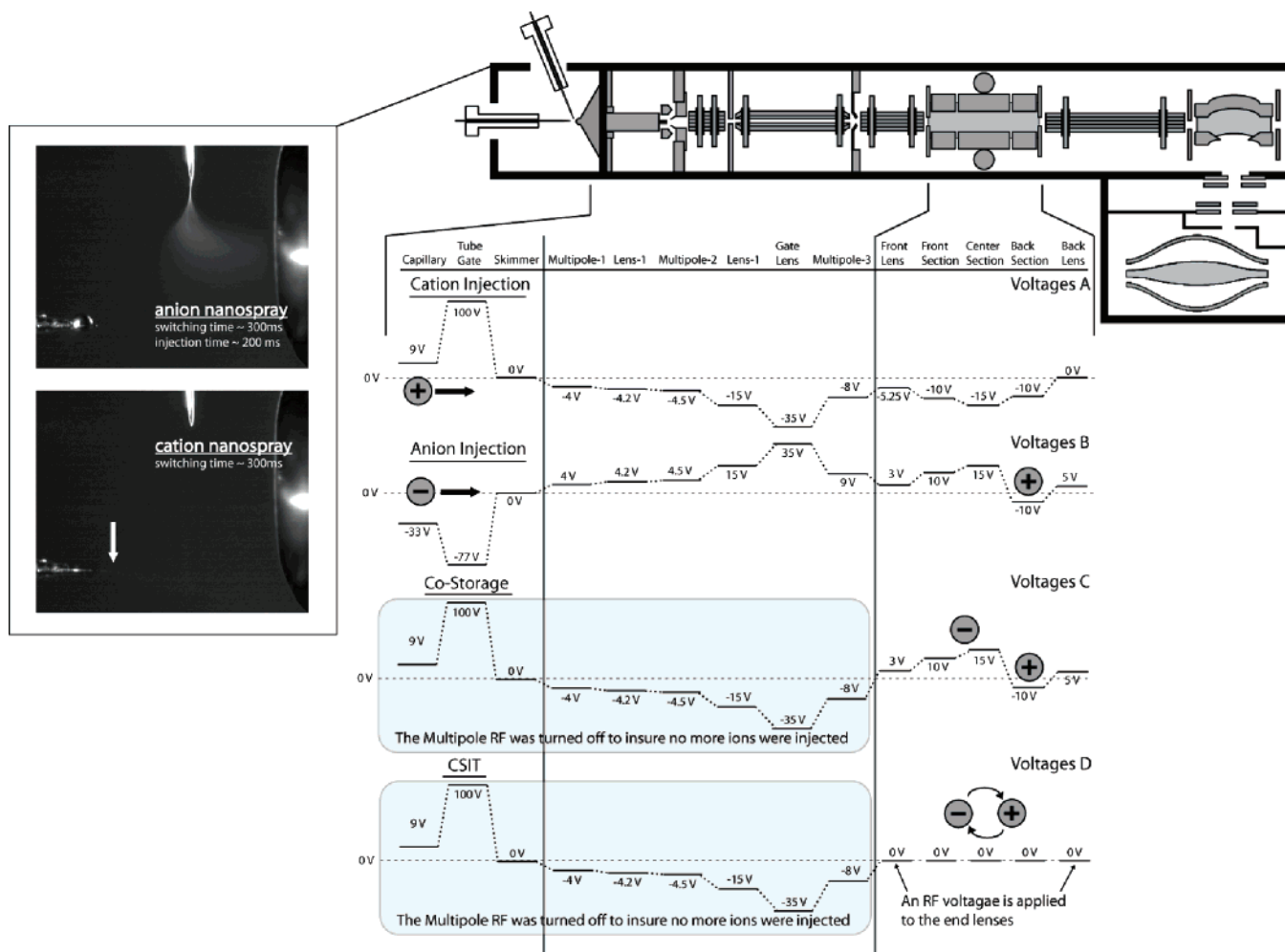


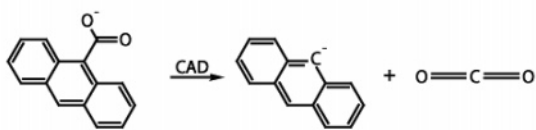
Figure 1. Schematic of the dual-nESI source and the QLT-orbitrap hybrid mass spectrometer. The lift-out panels highlight the pulsed, dual-nESI inlet and the associated ion optic, multipole, and trap section potentials during a typical FE-ETD scan. Note the orbitrap diagram was adapted from ref 16.

Cations were then injected and isolated using the same scheme employed by all the typical MS and MS/MS experiments (Figure 1, voltages A) on the hybrid system (i.e., CID and PQD). Following injection, a negative dc offset voltage was applied to the back section and the center section and front sections of the QLT were placed at a positive offset. The negative potential of the back section retained the cation precursor population in the QLT while the positive potentials of the front and center sections allowed the anion population to be injected. Note all potentials on the ion-transfer optics between the source and QLT were adjusted to pass negative ions at this time (Figure 1, voltages B). Next, the cation power supply was pulsed low (0 kV) and the anion power supply pulsed high (-0.7 to -2 kV). This adjustment extinguished the cation spray and initiated the anion spray. After 400 ms—the time needed to allow the power supply to reach the set point and the nanospray to settle—reagent anions were injected. Injection times of 200–300 ms were required to generate a sufficient reagent anion population for subsequent ETD reactions.

Following anion injection there was a period of costorage without mixing; i.e., the anion and cation populations were spatially segregated for ETD reagent anion preparation (Figure 1, voltages C). At this time, the rf voltages applied to the transfer multipoles were set to zero to prevent the injection of any more ions. To

allow the cation nanospray to settle before the beginning of the next injection event (0.5–2 s later depending upon which mass analyzer was used), the anion power supply was pulsed low and the cation power supply was pulsed high ($+0.7$ to 2 kV). Collision activation of the anion population was performed while both anion and cation populations were spatially segregated. The activation step utilized a wide window (10 m/z units) to compensate for space charge-induced nonideal ion behavior (Figure 2). To purify the reagent anion population, following collisional activation, a second isolation was performed using a notched waveform (to preserve both the desired anion and the precursor cation populations). Implementation of the notched waveform was somewhat particular. Wide cation notches prevent resonant excitation at the fringes of the ion cloud; however, wider notches also increase the probability of anion contaminants leaking through into the final ion mixture. Therefore, there is a tradeoff between pure anion reagent populations and unintended collisional activation of the cation precursor. Here, we elected to utilize a 45 m/z width cation notch to reduce the possibility of CAD-type fragmentation of the precursor cation. After isolation, the trap was adjusted to CSIT conditions (Figure 1, voltages D). Under these trapping conditions, the peptide and protein precursor cations react with the anionic reagents. To quench the reaction, the rf voltage on the end lenses

A) Reaction Scheme



B) Un-activated ETD precursor



C) Activated and Isolated ETD reagent

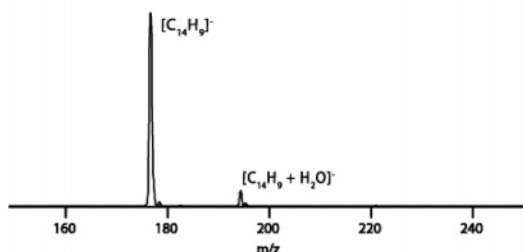


Figure 2. Reaction scheme for the conversion of 9-anthracenecarboxylic acid to an ETD reagent anion (A). Panel B displays the signal resulting from nESI of 9-anthracenecarboxylic acid, while panel C displays the decarboxylated post-CAD product.

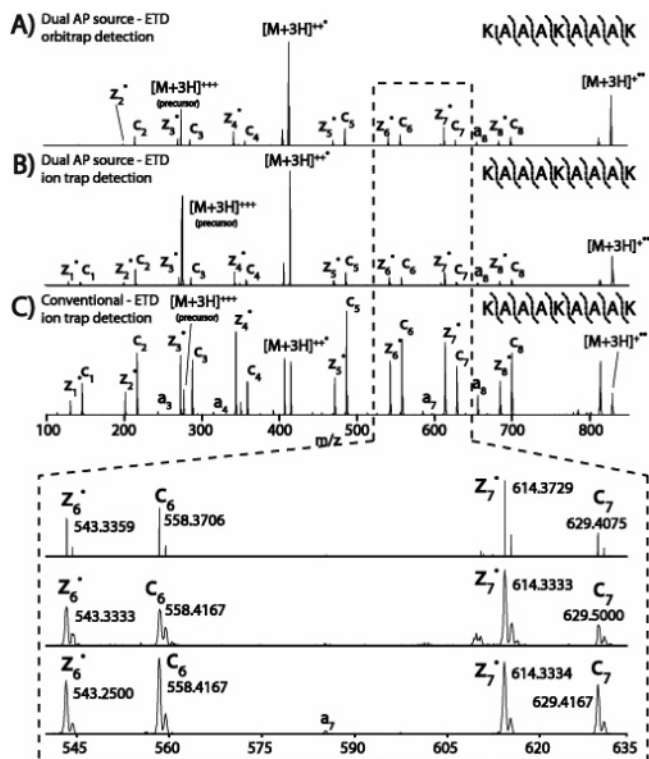


Figure 3. Three different ETD tandem mass spectra from the triply protonated synthetic peptide KAAAKAAK (each spectrum represents 10 single-scan spectra): FE-ETD with orbitrap mass analysis (A), FE-ETD with QLT mass analysis (B), and conventional ETD with rear injection of anions produced by a CI source and mass analysis using a QLT (C). The expanded region below highlights the heightened resolution achieved when using the orbitrap mass analyzer.

Table 1

fragments	(A) KAAAKAAK				
	theoretical	LIT	error (ppm)	orbitrap	error (ppm)
z ₂	202.1312	202.1	237	202.132	2.5
c ₂	217.1659	217.2	3.7	217.167	2.8
z ₃	273.1683	273.2	5.9	273.169	2.9
c ₃	288.2030	288.2	126.0	288.204	2.8
z ₄	344.2054	344.3	129.6	344.206	2.3
c ₄	359.2401	359.3	27.6	359.241	2.2
z ₅	472.3004	472.3	69.7	472.301	1.7
c ₅	487.3351	487.3	3.7	487.336	1.4
z ₆	543.3375	543.3	161.0	543.338	1.7
c ₆	558.3722	558.4	79.7	558.373	1.6
z ₇	614.3746	614.3	67.2	614.376	1.6
c ₇	629.4093	629.6	276.4	629.410	1.6
z ₈	685.4117	685.3	114.2	685.413	1.8
c ₈	700.4464	700.6	195.6	700.448	1.6
	(B) Substance P				
c ₂	271.1877	271.3	229.7	271.188	2.6
c ₈ ⁺²	523.7983	523.9	226.0	523.799	1.1
c ₉ ⁺²	552.3091	552.5	345.6	552.310	0.9
c ₁₀ ⁺²	608.8511	608.9	107.7	608.852	1.1
c ₅	624.3940	624.5	169.8	624.395	1.3
c ₆	752.4526	752.5	63.0	752.454	1.3
c ₇	899.5210	899.7	162.0	899.522	1.3
c ₈	1046.5894	1046.5	85.4	1046.590	0.4
c ₉	1103.6109	1103.7	50.6	1103.612	1.2
c ₁₀	1216.6949	1216.8	45.3	1216.697	1.4
	(C) Angiotensin				
c ₂	289.1619	289.3	304.7	289.161	1.7
c ₃	388.2303	388.3	50.7	388.230	2.1
z ₃	400.2105	400.3	98.7	400.210	2.0
c ₄	551.2936	551.4	223.3	551.292	2.9
z ₅	634.3222	634.3	113.8	634.321	2.2
c ₅	664.3777	664.3	66.8	664.376	3.3
z ₆	747.4062	747.3	97.4	747.404	2.7
c ₇	898.4894	898.6	104.6	898.487	2.8
z ₇	910.4696	910.3	241.2	910.467	2.6
z ₈	1009.538	1009.4	120.2	1009.535	2.7
c ₈	1045.5578	1045.5	55.3	1045.555	2.6
z ₉	1165.6391	1165.5	119.3	1165.636	3.1
c ₉	1182.6167	1182.6	28.2	1182.614	2.5
	(D) Averages				
	KAAAKAAK	SubP	ATCH		
error-LIT (ppm)	106.9	148.5	124.9		
error-orbitrap (ppm)	2.0	1.3	2.5		

was turned off and a negative potential was applied to the center section. The negative potential selectively ejects the negative ions while retaining the positive fragment ions. At this point, ion/ion reaction products were mass analyzed using either the QLT or the orbitrap.

Cellular Digestion and Liquid Chromatography. Yeast cells ("wild type" S288C strain, α mating type, diploid, *SUC2 mal mel gal2 CUP1*) were cultured on yeast nitrogen base (YNB; DIFCO, Detroit, MI) that lacked amino acids and ammonium sulfate but had additional glucose (2% v/v)—a loop was dipped into a 100-mL solution of 1.7 g/L YNB that lacked amino acids and ammonium sulfate, but had 4% glucose and 5 g of ammonium sulfate, and was adjusted to a pH of 5.6 using NaOH. The solution was shaken overnight at 30 °C. After ~18 h, this solution was transferred to a Fernboch and shaken for ~18 h at 30 °C. The resulting solution was spun down, washed with deionized water (DI H₂O), and then resuspended in a lysis buffer (50 mM Tris

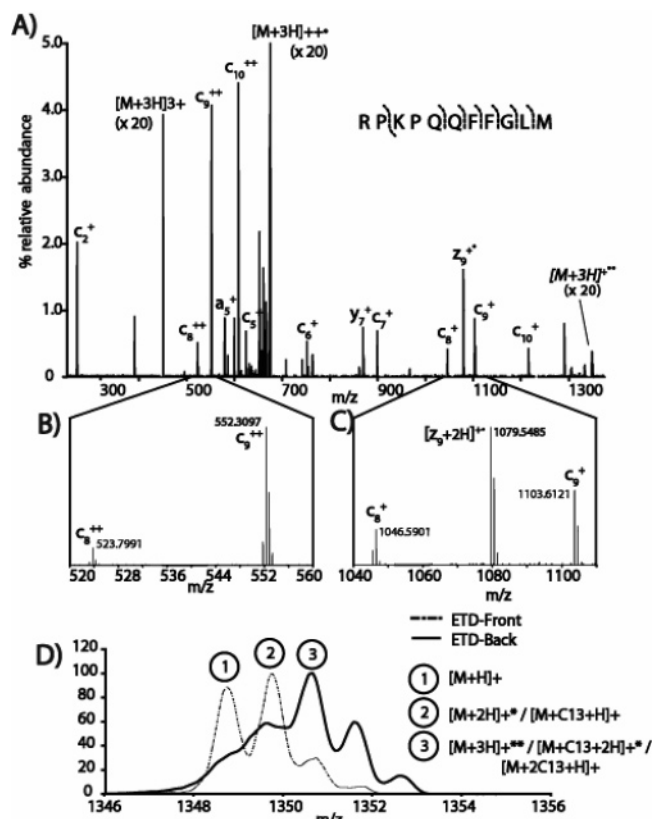


Figure 4. Ten averaged single-scan FE-ETD spectra of substance P (RPKPKQFFGLM-amide, A). Panels B and C display expanded regions and the resolution of the c_8 and c_9 product ions. Panel D was produced using the same reaction conditions, but with m/z analysis in the QLT. Panel D displays the m/z range of the charged-reduced precursor isotope cluster, for FE-ETD and conventional ETD, respectively. The shift in the isotopic ratio from low to high m/z for FE-ETD to conventional ETD is indicative of a shift from PTR to ET-type reactions.

base, 0.3 M sucrose, 5 mM Na_2EDTA , 1 mM EDTA-free acid, 1 mM PMSF from 100 mM IPA stock, pH to 7.5 with HCl). For lysis, the yeast cells were sonicated in 1-min intervals for a total of ~ 3 min. Organelles and membranes were pelleted using centrifugation ($\sim 2000g$ and $\sim 100000g$, respectively). After an acetone precipitation, the soluble proteins were resuspended in 6 M guanidinium hydrochloride (GHCl). The protein extracts were equally aliquoted and digested with Lys-C (0.5 M GHCl for ~ 18 h at pH ~ 8).

For the liquid chromatography tandem MS analysis, ~ 8 pmol of yeast digest was bomb loaded onto a $360 \mu\text{m} \times 75 \mu\text{m}$ self-prepared microcapillary precolumn, which was fritted (Lichrosorb Si60, EM Separations Technology, Gibbstown NJ) and packed in-house with reversed-phase C_{18} material to 5 cm (Alltima $5\text{-}\mu\text{m}$ beads from Alltech Associates, Inc., Deerfield IL). A separate $360 \mu\text{m} \times 50 \mu\text{m}$ microcapillary column was attached to the precolumn—also packed with 7 cm of reversed-phase C_{18} material—with a Teflon tubing butt joint. The second column had an integrated ESI tip, made using a laser puller (model P-2000, Sutter Instrument Co., Novato, CA).²¹ A nanoflow organic solvent gradient was run over these attached columns using an Agilent

(21) Martin, S. E.; Shabanowitz, J.; Hunt, D. F.; Marto, J. A. *Anal. Chem.* **2000**, *72*, 4266–4274.

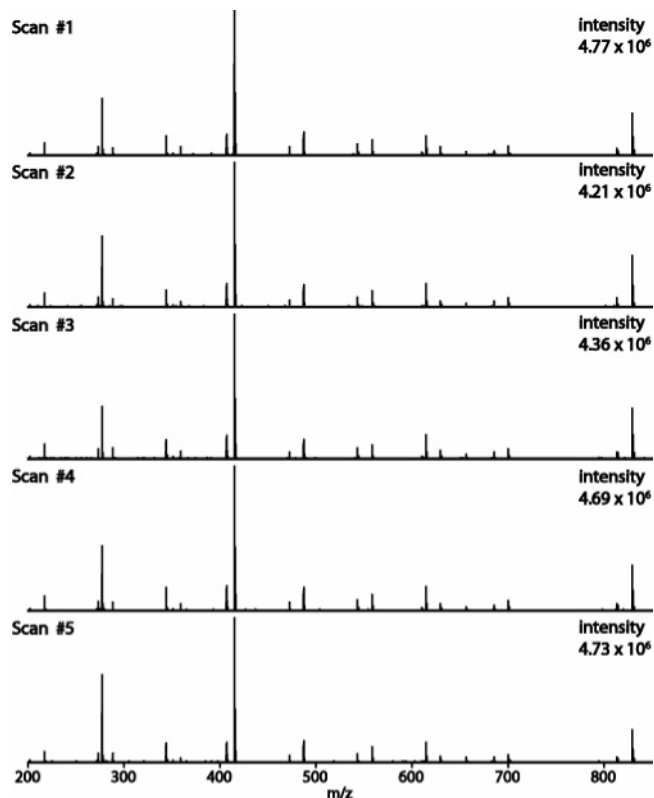


Figure 5. Five consecutive single-scan FE-ETD spectra (with orbitrap m/z analysis) of the triply protonated KAAAKAAK peptide. Both the overall intensity and intensity of the individual fragment ions is consistent across all five spectra.

1100 series HPLC and a micro-T for flow splitting (Agilent Technologies, Palo Alto, CA). A 65-min gradient was used to separate the peptides. Solvent A consisted of 100 mM aqueous acetic acid. Solvent B consisted of 70:30 acetonitrile/water with 100 mM acetic acid. The gradient began with 100% A, but then went to 70:30 A/B in 1 min. Next, the gradient was increased linearly over the next 44 min to 60% B. The system held at 40:60 for 15 min, and then it made a final push to 100% B over the last 5 min.

RESULTS AND DISCUSSION

Figure 1 displays the sequence of events for a typical experiment. Cations are injected first, followed by precursor selection, isolation, and storage in the rear segment of the QLT. Immediately following, the ion-transfer optic voltages are reversed, the cation spray voltage is removed, and the anion spray voltage is applied. Once a stable anion spray is initiated, anionic reagents are injected into the middle section of the QLT. Next, the anion population (deprotonated 9-anthracenecarboxylic acid, m/z 221) is collisionally activated and dissociates via decarboxylation to yield a product ion of m/z 177 (Figure 2). As recently demonstrated by McLuckey et al., this anion is capable of inducing ETD and is the major product of activation. The anion reagent population was then purified using an isolation waveform (Figure 2B). Superposition of rf on the end trapping lenses and removal of the dc offset voltages on the three segments of the QLT allow CSIT and, consequently, ion/ion chemical reactions. Following the reaction, product ions were mass analyzed using either the QLT or orbitrap.

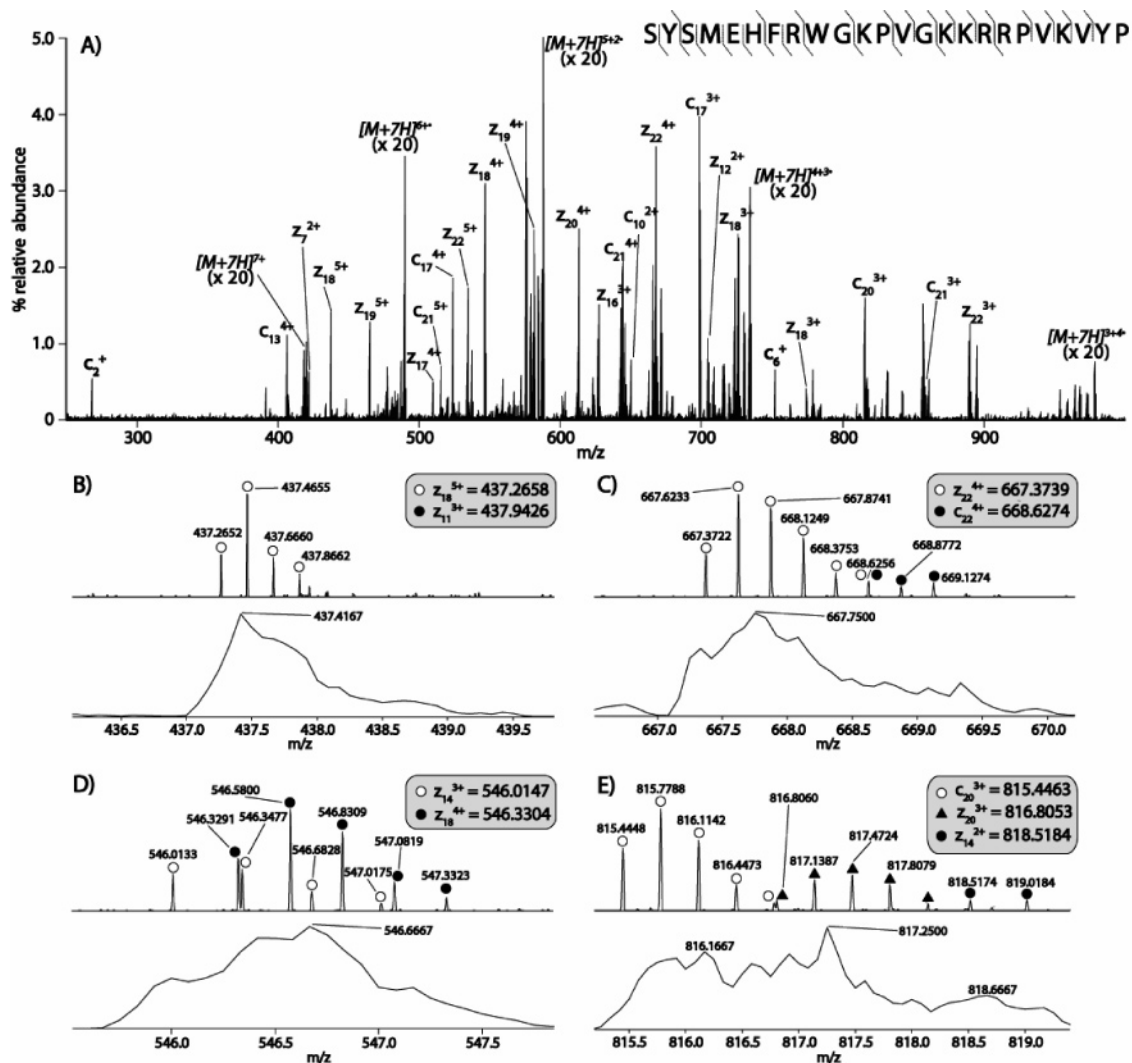


Figure 6. Ten averaged single-scan FE-ETD spectra of the ATCH peptide performed using orbitrap mass analysis. The upper portion of panels B–E display expanded regions of the entire spectrum shown in panel A, while the lower region displays the FE-ETD result achieved when using the lower resolution QLT for m/z analysis.

Our initial experiments reacted a triply protonated synthetic peptide (KAAAKAAAK) with the decarboxylated 9-anthracenecarboxylic acid anion (m/z 177) for 100 ms. Figure 3 displays the results of that reaction following m/z analysis using either the orbitrap (Figure 3A) or the QLT (Figure 3B); each spectrum represents the average of 10 single-scan mass spectra, which required ~ 30 s to collect. For comparison, the same peptide was dissociated using the more conventional fluoranthene radical anion. Note this experiment was performed on a separate QLT instrument that had been modified to inject anions generated via NCI through the back side of the trap. In all cases, a complete or near-complete series of c- and z-type product ions was generated. We also noted a decreased relative intensity of c- and z-type products ions relative to the charge-reduced product ions when using the ESI-generated anion. This decrease in ETD efficiency was observed when using either the orbitrap (Figure 3A) or QLT (Figure 3B) for m/z analysis. Thus, we conclude the ESI-derived anion used here is less efficient than the more common fluoranthene radical anion (see below for a detailed description). The inset of Figure 3 displays the greatly enhanced m/z resolution achieved by collecting spectra in the orbitrap as compared to the

QLT. Table 1A presents the measured and theoretical mass accuracies for all detected c- and z-type product ions for this experiment. Using the orbitrap, the m/z values of the observed product ions were always measured to within 3 ppm of their theoretical values.

To characterize the ETD efficiency of the ESI-generated anion, we analyzed the benchmark ECD standard peptide, substance P (RPKPQQFFGLM-amide, Figure 4). Ion/ion reactions result from the formation of a long-lived cation–anion orbiting complex.^{12,22,23} Once formed, there are two main reaction pathways: (1) the anion can donate an electron to the cation, or (2) the anion can abstract a proton from the cation. For the case of electron donation, the radical cation often dissociates (i.e., ETD). Evidence of ETD can be found in the extensive series of c- and z-type product ions that are observed following reaction of the triply protonated substance P with the ESI-generated reagent anion. However, these species occur at a relative abundance of 1–5% of the charge-reduced

(22) Stephenson, J. L.; VanBerkel, G. J.; McLuckey, S. A. *J. Am. Soc. Mass Spectrom.* **1997**, *8*, 637–644.

(23) Stephenson, J. L.; McLuckey, S. A. *J. Am. Chem. Soc.* **1996**, *118*, 7390–7397.

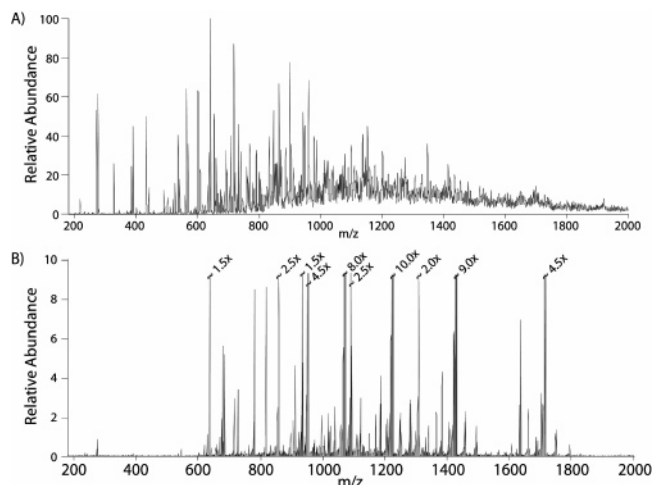


Figure 7. ETD product ion spectra of ubiquitin using conventional ETD (i.e., rear injected reagent anions produced by a CI source and mass analyzed with a QLT, A) or FE-ETD (i.e., reagent anions produced by pulsed ESI and mass analyzed with an orbitrap, B). The predominance of the charge-reduced molecular ion peaks over the c- and z-type fragment ions in the ESI-generated anion spectra is indicative of the low ETD efficiency of that anion. But, interrogation by conventional ETD results in a wide range of dissociation pathways as seen in the large variety of product ions.

peaks. Figure 4A has been magnified 5 times to make these peaks observable. Panel D of Figure 4 displays an inset of the precursor ion m/z range following two charge reduction reactions with either the ESI-generated anion or the radical anion of fluoranthene. The product ions represented by these peaks are the result of one of the following: two-proton transfer ($[M + H]^+$), one-proton transfer and one-electron-transfer events ($[M + 2H]^+$), or two-electron transfers ($[M + 3H]^{2+}$). Deconvolution of the isotopic distributions into the contributing species is one approach to estimating the partitioning between proton and electron transfer for each of these reagent anions. We used linear algebraic equations based on the theoretical isotopic contributions of all potential products to determine that the ESI-generated anion of m/z 177 had a $\sim 7:1$ ratio of PTR/ET, while the radical anion of fluoranthene had a $\sim 1:3$ ratio. This calculation excludes electron-transfer reactions that result in dissociation and neglects the contribution of hydrogen atom loss resulting from ET. The calculation, however, provides a good measure of the extent of PTR—which is the apparent cause of the relatively low efficiency of the ESI-generated ETD reagent anion.

A second method of measuring a reagent anion's propensity to induce electron transfer has been defined by McLuckey et al. as % ETD—the intensity of ETD-derived product ions over the total product ion intensity.²⁴ We have altered this method to also include the nondissociative electron-transfer events (ET), thus defining % ETD + ET. For the triply protonated substance P precursor, the fluoranthene radical anion yielded a % ETD + ET ratio of 65.4%, while the ESI-derived anthracene anion yielded only 16.9%. Despite the relatively low efficiency of the ESI-generated anion to induce ET/ETD, the injection scheme and scan sequence reported here is reproducible and robust. Figure 5 shows five consecutive single-scan MS/MS spectra (w/ orbitrap mass

analysis) resulting from reaction of the ESI-generated anion (m/z 177) with the triply protonated KAAAKAAAK peptide. Each spectrum was collected in ~ 3 s and coordinates well with its neighbors.

Even with its low efficiency, the ESI-generated ETD reagent anion proved useful, especially when coupled with the orbitrap mass analyzer to characterize large, highly charged peptide and protein precursor cations. A 30-ms ETD reaction of septuply protonated ATCH peptide (SYSMEHFRWGKPVGKK-RRPVKVP) followed by orbitrap m/z analysis illustrates this point (Figure 6A, 10 single-scan spectra, ~ 30 -s collection period). Due to space limitations, not all of the c- and z-type ion peaks were labeled—all observed cleavages, however, are denoted on the sequence at the top the figure. Despite the lower anion densities and reaction efficiencies of the ESI-generated ETD reagent anion (relative to fluoranthene), there is still good sequence coverage. The main reason for this is the relative ease of identifying fragments. With the high-mass accuracy and resolving power of the orbitrap, fragments that approach the 3:1 signal-to-noise ratio can be identified very comfortably. Many of these identifications could not be made on spectra collected with a QLT. Product ion assignment for a precursor of this size and charge is extremely dubious when m/z analysis is performed with a QLT due to low m/z resolution and accuracy. Figure 6, panels B–D, highlight selected instances where the orbitrap was necessary for fragment ion identification. In panel B, there are two different theoretical z-type fragment possibilities— z_{18}^{+5} (m/z 437.2658) or z_{11}^{+3} (m/z 437.9426). The resolution of the QLT does not allow charge-state identification, so distinguishing these two possibilities is difficult. Mass-to-charge analysis using the orbitrap resolves the charge state as a +5 and measures the m/z value to within 1.4 ppm of the z_{18}^{+5} . Panel C demonstrates the ability of the orbitrap to distinguish two overlapping isotopic cluster peaks from the z_{22}^{+4} and c_{22}^{+4} ions. Using the QLT, the z_{22}^{+4} could tentatively be assigned, but identification of c_{22}^{+4} is ambiguous at best. Panel D demonstrates the resolution of two overlapping product ion m/z peaks using the orbitrap. In this case, an unresolved peak is observed during QLT analysis; however, there is no way to determine from which fragment the peak arose. Finally, panel E displays the identification of three distinct c- and z-type product ions in a 3.5 m/z window using the orbitrap for mass analysis.

Beyond greatly increased resolving power, performing mass analysis with the orbitrap results in significantly increased m/z accuracy for ETD product ions as compared to the QLT. Table 1 highlights the improvement in m/z accuracy between the two mass analyzers. c- and z-type product ions are routinely measured to within 3 ppm using the orbitrap (with external calibration), while the QLT achieves ~ 125 ppm. The key benefit from this increased mass accuracy is the confidence with which fragment ions can be identified. This is true for both manual identification (described above) and when using automated analysis software. ProSight PC is an automated analysis program that was developed by Kelleher et al. to perform database searching of tandem mass spectra collected with FT-ICR-MS systems.^{25–29} ETD tandem mass spectra collected using the orbitrap are directly compatible with

(24) Pitteri, S. J.; Chrisman, P. A.; Hogan, J. M.; McLuckey, S. A. *Anal. Chem.* **2005**, *77*, 1831–1839.

(25) Meng, F. Y.; Cargile, B. J.; Miller, L. M.; Forbes, A. J.; Johnson, J. R.; Kelleher, N. L. *Nat. Biotechnol.* **2001**, *19*, 952–957.

(26) Taylor, G. K.; Kim, Y. B.; Forbes, A. J.; Meng, F. Y.; McCarthy, R.; Kelleher, N. L. *Anal. Chem.* **2003**, *75*, 4081–4086.

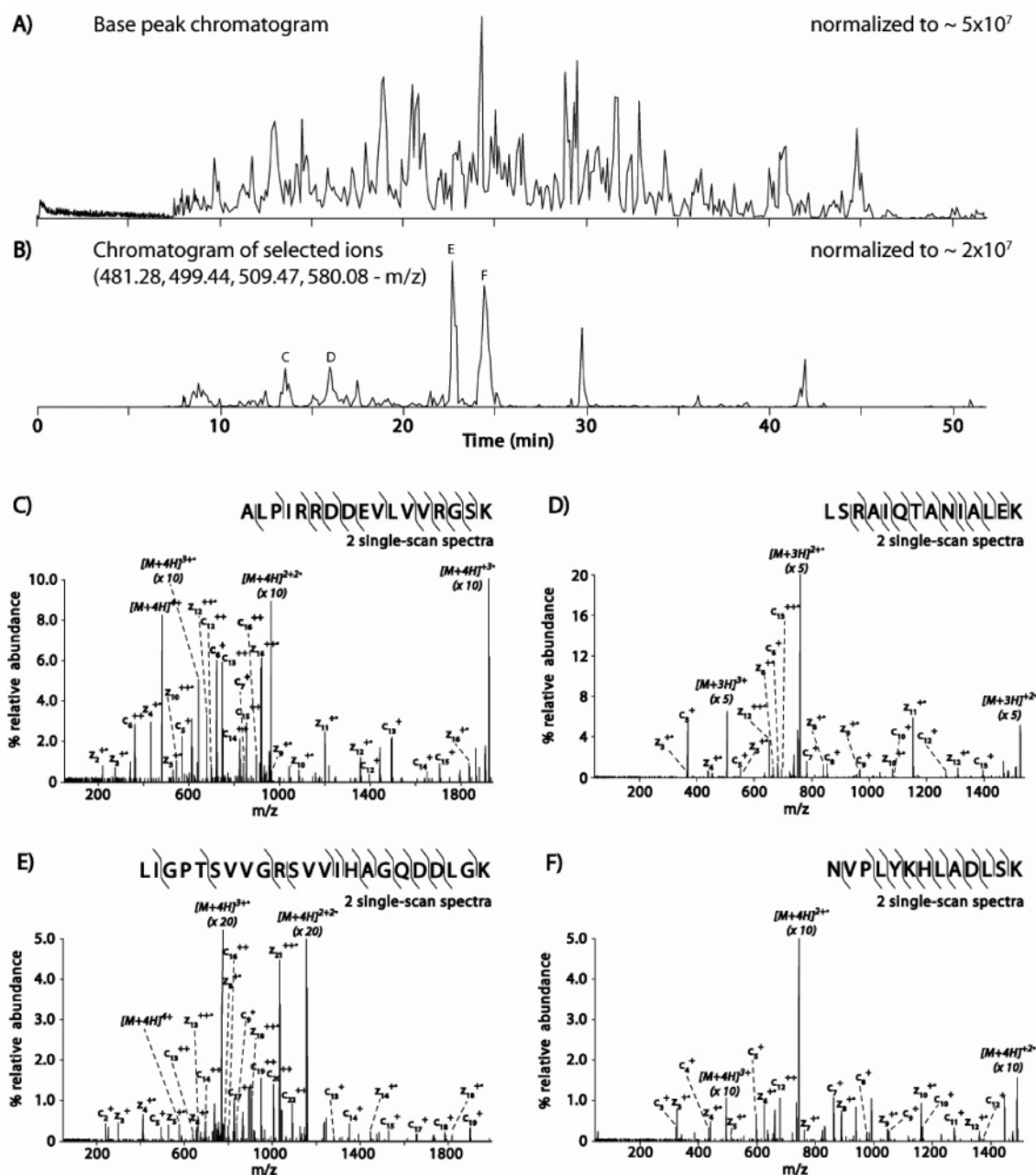


Figure 8. nHPLC-MS analysis of a Lys-C digested yeast whole protein sample. An automated data-dependent analysis was designed to first analyze the eluent by full-MS using the orbitrap mass analyzer followed by two averaged FE-ETD scans of the most intense ion having at least three charges from the full scan. Panel A displays the base peak chromatogram, while panel B shows the selected ion chromatogram of m/z values 481.22, 499.44, 509.47, and 580.08. Panels C–F display MS/MS spectra resulting from ETD fragmentation of those precursor m/z values.

ProSight PC because the m/z resolution and accuracy are comparable to that achieved using FT-ICR-MS systems. Additionally, Kelleher and co-workers have recently modified this program to accommodate low-resolution ETD-MS/MS data collected on a standalone QLT. Thus, using ProSight PC, we can directly compare how ETD tandem mass spectra collected at low and high m/z resolution affect the outcomes of an automated analysis.

- (27) LeDuc, R. D.; Taylor, G. K.; Kim, Y. B.; Januszyk, T. E.; Bynum, L. H.; Sola, J. V.; Garavelli, J. S.; Kelleher, N. L. *Nucleic Acids Res.* **2004**, *32*, W340–345.
- (28) Pesavento, J. J.; Kim, Y. B.; Taylor, G. K.; Kelleher, N. L. *J. Am. Chem. Soc.* **2004**, *126*, 3386–3387.
- (29) Roth, M. J.; Forbes, A. J.; Boyne, M. T.; Kim, Y. B.; Robinson, D. E.; Kelleher, N. L. *Mol. Cell. Proteomics* **2005**, *4*, 1002–1008.

To evaluate the affect of m/z resolution, intact ubiquitin cations were isolated (+13, m/z 659) and analyzed in three ways: (1) reacted with fluoranthene anions generated via NCI and m/z analyzed in the QLT (standalone system), (2) reacted with the ESI-generated anion of m/z 177 and mass analyzed using either the orbitrap or (3) the QLT (Figure 7; each spectrum represents ~40 single-scan spectra, which required 2 min to collect). The predominance of the charge-reduced molecular ion peaks over the c- and z-type fragment ions in the ESI-generated anion spectra is indicative of the low ETD efficiency of that anion. ProSight PC search parameters varied depending upon data quality—e.g., mass tolerances were set at 0.5 Da for spectra collected with the QLT and 0.050 Da for orbitrap data. Indicative of the poor ETD

efficiency of the ESI-generated reagent, ProSight PC could not identify ubiquitin (the ubiquitin sequence was inserted into an Arabidopsis database) from the QLT-acquired spectra; however, when the orbitrap was used for m/z analysis, the high m/z resolution and accuracy compensates for the low ETD efficiency, resulting in a high probability match to the correct sequence—probability score (P -score) of 3.92×10^{-26} and an expectation score (a scaled P -score) of 1.31×10^{-20} . The higher efficiency ETD spectra of the same protein, using fluoranthene anions injected from the back, but with m/z analysis on a QLT resulted in a P -score of 3.00×10^{-13} and an expectation score of 1.01×10^{-7} .

We note the identified fragments of the two successful searches were quite different. Due to the lower resolving power of the QLT, analysis of the fluoranthene-generated spectra only produced identifications for fragment ions with a single charge. This limitation, in conjunction with the QLT's upper m/z limit of 2000, meant that only N and C terminal fragments up to 16 residues in length could be identified. Any other fragments were either too big or too highly charged. Previous work, by us and others, has demonstrated that such complicated spectra can be simplified by subjecting the product ions to sequential proton-transfer ion–ion reactions.^{7,30} For lower resolution instruments such as the QLT, this step concentrates the terminal fragments in the single charged state and moves overlapping highly charged fragments beyond the scanned m/z range. Such spectral simplification can help to bolster the probability and expectation scores of the identification, but it would not result in identifications of fragment ions that were longer than ~ 16 residues.

Because multiply charged fragments are easily resolved using the orbitrap, fragments spanning the whole length of the protein were identified in the ESI-generated ETD reagent anion spectra. Ultimately, this additional resolving power translates into more positive identifications and better sequence coverage—for the case of these two searches, 46 fragments were identified in the orbitrap data while only 21 were identified in the QLT data. In this instance, using either the QLT or orbitrap for ETD product ion analysis results in the correct identification. The N and C terminal sequence tags procured by the ETD-PTR approach are more than sufficient for protein identification. Mass analysis using orbitrap, however, can provide coverage across the entire protein and allow for the precise location of PTM motifs or the location of alternative splice sites, etc.

Scan time, duty cycle, and stability are figures of merit that are important to any mass spectrometric method as good performance in these areas can permit higher order experiments such as coupling with online chromatographic separations. To assess the compatibility of FE-ETD with chromatography, we analyzed a complex mixture of LysC-generated peptides from a yeast whole-cell extract. The digested peptides were separated by nHPLC (Figure 8A) using a data-dependent method that first analyzed all eluting species by performing a full-scan MS in the orbitrap. Next, the most intense peak was dissociated using our FE-ETD method followed by product ion mass analysis in the

orbitrap (two single-scan spectra were averaged for each MS/MS event, ~ 6 s). From this run, 34 unique peptides were identified following an automatic database search using ProSight PC. Figure 8C–F highlights selected spectra and the associated ProSight PC ID. For comparison, the same sample was analyzed by LC–MS/MS with a conventional ETD setup, which injected fluoranthene ions into the back of the trap and used a QLT for m/z analysis. From these data, 1031 unique peptides were identified. We note, however, that each FE-ETD scan required ~ 20 -fold more time to complete than a conventional ETD event. This fact, and the high dynamic range of the sample, account for the low number of FE-ETD identifications. Notwithstanding, these data demonstrate the overall reliability of the pulsed ESI FE-ETD approach and compatibility with automated data acquisition. At present, the main limiting factor of the FE-ETD approach is the relatively long times required for anion injection and the low efficiency of the FE-ETD anion. Doubtless significant room for optimization remains for both of these parameters.

CONCLUSIONS

The acquisition of ETD product ion spectra on high resolving power instrumentation is of obvious importance to the field of proteomics. Here we have described the implementation of FE-ETD using dual, pulsed nESI sources. The main strength of this approach is the relative simplicity and ease with which it can be performed. Overall, we find the approach to be reliable and robust—even permitting coupling with online chromatographic separations. Fairly long pulsing times and relatively low ET efficiency, as compared to conventional ETD, are the main drawbacks of the FE-ETD approach. We note more rapid methods of pulsing dual nESI probes have been described and could easily be adapted for this application.³² Still the value of such a system for large peptide and whole protein analysis was readily apparent for the characterization of the standard protein ubiquitin. c- and z-type fragment ions that were not identifiable using QLT, even in the more efficient conventional ETD format, were easily identified by ProSight PC from the FE-ETD data, resulting in increased sequence coverage and higher probability scores. These results suggest that the implementation of ETD on sensitive, high-resolution, and high-mass accuracy hybrid instrumentation, such as the orbitrap, will substantially propel the emergent fields of middle- and top-down proteomics. Finally, we note the combination of improved mass accuracies (generally < 2 ppm) and near-complete fragmentation afforded by ETD will help drive the development of reliable, automated de novo data interpretation algorithms.³¹

ACKNOWLEDGMENT

The authors thank the University of Wisconsin—Madison, the WiCell Research Institute, Thermo Electron, and the National Institutes of Health (R01GM080148 to J.J.C.) for financial support of this work. We also thank Jae Schwartz and George Stafford for helpful discussions; Michael Sussman for donation of the yeast cell lysate; and Neil Kelleher, Rich LeDuc, and Craig Wenger

(30) Badman, E. R.; Chrisman, P. A.; McLuckey, S. A. *Anal. Chem.* **2002**, *74*, 6237–6243.

(31) Savitski, M. M.; Nielsen, M. L.; Kjeldsen, F.; Zubarev, R. A. *J. Proteome Res.* **2005**, *4*, 2348–2354.

(32) Nepomuceno, A. I.; Muddiman, D. C.; Bergen, H. R.; Craighead, J. R.; Burke, M. J.; Caskey, P. E.; Allan, J. A. *Anal. Chem.* **2003**, *75*, 3411–3418.

for invaluable assistance with ProSight PC. Finally, G.C.M. and D.M.G. gratefully acknowledge support from an NIH predoctoral fellowship—Biotechnology Training Program (NIH 5T32GM08349).

Received for review January 3, 2007. Accepted March 20, 2007.

AC070020K